

# Skyrme model on $S_3$ and Harmonic maps

Y. Brihaye<sup>◊</sup> and C. Gabriel <sup>\*†</sup>

<sup>◊</sup>Dep. of Mathematical Physics, University of Mons-Hainaut, Mons, Belgium

<sup>†</sup>Dep. of Mechanics and Gravitation, University of Mons-Hainaut, Mons, Belgium

## Abstract

A non-linear sigma model mimicking the Skyrme model on  $S_3$  is proposed and a family of classical solutions to the equations are constructed numerically. The solutions terminate into catastrophe-like spikes at critical values of the Skyrme coupling constant and, when this constant is zero, they coincide with the series of Harmonic maps on  $S_3$  constructed some years ago by P. Bizon.

## 1 Introduction

A few years ago P. Bizon [1] constructed a remarkable sequence of harmonic maps from  $S_3$  into  $S_3$ . Only a few examples are known of non-linear equations which admit such a sequence of regular solutions. Some of them occur in the framework of gauged non-linear sigma models. The prototype of non-linear sigma model in theoretical physics is the Skyrme model [2]. It is based on a mapping of the physical space  $\mathbb{R}^3$  into the manifold of the Lie group  $SU(2)$ , which is homeomorphic to  $S_3$ . In order to guarantee the existence of topological soliton the physical space is compactified. The original Skyrme model possess an  $SU(2) \otimes SU(2)$  global symmetry which can partly be gauged. Several examples of sequence of regular-finite energy classical solutions appear in different gauged versions of the Skyrme model [3, 4].

---

<sup>\*†</sup> Aspirant F.N.R.S

For all known examples, an interesting phenomenon, related to catastrophe theory, occurs to the solutions when the minimal (i.e. quadratic in the derivatives) sigma model is supplemented by a quartic term in the derivatives [5, 4, 6], a so called Skyrme term. The higher derivative interaction term is proportional to a free constant, say  $\epsilon$ , which constitutes a coupling constant of the model. To be more concrete let us denote (in the models [5, 4, 6]) by  $S_n(\vec{x}, \epsilon = 0)$ ,  $n \in \mathbb{N}$  the sequence of solutions available in absence of the Skyrme term and  $E_n(0)$  the corresponding classical energy. Solving the classical equations for  $\epsilon > 0$ , it appears that a branch of solutions  $S_n(\vec{x}, \epsilon)$  exists for  $0 \leq \epsilon \leq \epsilon_{cr}(n)$  and that no solution is available for  $\epsilon > \epsilon_{cr}(n)$ . However, there exists a second branch of solution, say  $\tilde{S}_n(\epsilon)$ , for  $\epsilon \in ]0, \epsilon_{cr}(n)[$ . The numerical results indicate that the following properties hold for  $n \in \mathbb{N}$

$$\tilde{E}_n(\epsilon) < E_n(\epsilon) \quad (1)$$

$$\lim_{\epsilon \rightarrow \epsilon_{cr}(n)} \tilde{E}_n(\epsilon) = E_n(\epsilon) \quad (2)$$

$$\lim_{\epsilon \rightarrow 0} \tilde{E}_n(\epsilon) = E_{n-1}(\epsilon) \quad (3)$$

In fact the statement (2) is even stronger because we have in fact

$$\lim_{\epsilon \rightarrow \epsilon_{cr}(n)} S_n(\vec{x}, \epsilon) = \lim_{\epsilon \rightarrow \epsilon_{cr}(n)} \tilde{S}_n(\vec{x}, \epsilon) = S_n(\vec{x}, \epsilon_{cr}(n)) \quad (4)$$

in a uniform sense for  $\vec{x} \in \mathbb{R}^3$ . The counterpart of Eq.(4) related to the limit (3) does not hold because the solutions  $S_n(\vec{x}, \epsilon)$  and  $S_{n-1}(\vec{x}, \epsilon)$  do not in general obey the same boundary conditions.

The plot of the energies  $E(n, \epsilon)$  and  $\tilde{E}(n, \epsilon)$  as a function of  $\epsilon$  shows that the two curves terminate at  $\epsilon = \epsilon_{cr}(n)$  into a cusp, characteristic of catastrophe theory.

This phenomenon is absent in the normal (i.e. ungauged) Skyrme model but it occurs in several gauged versions of this model, namely in the “hidden gauge” Skyrme model [7]. In passing let us point out that the trivial topological sector of the “hidden gauge” Skyrme model is equivalent to the (bosonic part of the) electroweak standard model considered in the limit of an infinitely heavy Higgs particle (i.e. for  $M_H \sim \lambda \rightarrow \infty$ ) [5, 4].

Owing the above properties associated with sequences of classical solutions available in the gauge-Skyrme model, it is natural to study how the harmonic maps of Ref [1] respond to the addition of a Skyrme interaction term. This is the aim of this paper.

## 2 The model

The functional energy studied in [1] reads

$$E_0(f) = \int_{S_3} h_{AB}(f) \frac{\partial f^A}{\partial x^i} \frac{\partial f^B}{\partial x^j} g^{ij} dV \quad (5)$$

where  $f$  represents a mapping from  $S_3$  (with local coordinates noted  $x^i$ ) into  $S_3$  (with local coordinates note  $f^A$ ). We use the same notations as in [1], namely  $x^i = (\psi, \theta, \phi)$  are the standard coordinates on  $S_3$  with the metric

$$ds^2 = d\psi^2 + \sin^2 \psi (d\theta^2 + \sin^2 \theta d\phi^2) \quad (6)$$

and similarly  $f^A = (\Psi, \Theta, \Phi)$  on the  $S_3$  target space.

The functional  $E_0(f)$  is a non-linear sigma model; the classical solutions, i.e. the extremum of the functional, are called harmonic maps in mathematics. In this paper, we study the extremum of the extended energy functional

$$E(f) = E_0(f) + E_{Sk}(f) \quad (7)$$

with the Skyrme interaction term

$$E_{Sk}(f) = \int_{S_3} h_{AB}(f) h_{CD}(f) \frac{\partial f^A}{\partial x^i} \frac{\partial f^B}{\partial x^j} \frac{\partial f^C}{\partial x^k} \frac{\partial f^D}{\partial x^l} (\mu_1 g^{ij} g^{kl} + \mu_2 g^{il} g^{jk}) dV \quad (8)$$

where  $\mu_1, \mu_2$  are constants. In order to keep the model (8) as close as possible to the standard Skyrme model defined on  $\mathbb{R}^3$  we choose  $\mu_1 = -\mu_2 \equiv \kappa^2$ .

Finally, we also assume that the function  $f^A(x^i)$  is equivariant i.e. invariant under the  $SO(3)$  rotations corresponding to the angles  $\theta$  and  $\phi$ . This leads us to the ansatz

$$\Psi(\psi) = f(\psi) \quad , \quad \Theta = \theta \quad , \quad \Phi = \phi \quad (9)$$

in terms of which the functional  $E(f)$  reads

$$E(f) = 4\pi \int_0^\pi \left\{ \sin^2 \psi \left( \frac{df}{d\psi} \right)^2 + 2 \frac{\sin^2 f}{\sin^2 \psi} + \kappa^2 \left( \frac{\sin^2 f}{\sin^2 \psi} \left( \frac{df}{d\psi} \right)^2 + \frac{\sin^4 f}{2 \sin^4 \psi} \right) \right\} d\psi \quad (10)$$

The classical equations are obtained by varying  $E(f)$  with respect to  $f$ . We are interested by solutions such that the energy density (i.e. the term in

bracket in the integral above) is regular. This imposes in particular  $f(0) = f(\pi) = 0$ .

In the purpose of comparison with the normal Skyrme model on  $\mathbb{R}^3$  we just write the expression of the classical energy in this model:

$$E(f) = 4\pi \int_0^\infty r^2 \left\{ \left( \frac{df}{dr} \right)^2 + 2 \frac{\sin^2 f}{r^2} + \kappa^2 \left( \frac{\sin^2 f}{r^2} \left( \frac{df}{dr} \right)^2 + \frac{\sin^4 f}{2r^4} \right) \right\} dr \quad (11)$$

### 3 The numerical solutions

It is convenient to label the extrema of the functional (10) by  $f_n(\psi, \kappa^2)$ , where the integer  $n$  counts the number of times the solution crosses the line  $f = \frac{\pi}{2}$ . It is also useful to notice the discrete invariances of the equation :

$$f(\psi) \rightarrow f(\pi - \psi) \quad , \quad f(\psi) \rightarrow \pi - f(\pi - \psi) \quad . \quad (12)$$

They transform any solution into another one with the same energy.

In [1] a sequence of extrema  $f_n(\psi, 0)$  (also called critical maps) to the functional (5) was constructed. It is such that  $f_0(\psi, 0) = 0$ ,  $f_1(\psi, 0) = \psi$ . To our knowledge, the solutions corresponding to  $n > 1$  cannot be expressed in terms of known functions. The profiles of the functions  $f_2(\psi, 0)$  and  $f_3(\psi, 0)$  are represented on Fig.1 and Fig.2 respectively. For the first few values of  $n$ , the energies are given [1] in the table below :

n	$E(n)/6\pi^2$
0	0
1	1
2	1.2319
3	1.3036
4	1.3240

We now discuss the evolution of these solutions for  $\kappa^2 \neq 0$ . Obviously the vacuum solution  $f_0 = 0$  (or, by (12),  $f_0 = \pi$ ) exists for all values of  $\kappa^2$  and its energy is zero. The solution corresponding to  $n = 1$  reads

$$f_1(\psi, \kappa^2) = \psi \quad \text{or} \quad f_1(\psi, \kappa^2) = \pi - \psi \quad (13)$$

and, like the vacuum, also exists irrespectively of the constant  $\kappa^2$ . It has an energy

$$E_1(\kappa^2) = 6\pi^2\left(1 + \frac{\kappa^2}{2}\right) \quad (14)$$

Solving numerically the equations for finite values of  $\kappa^2$  we find that the solution  $f_n(\psi, 0)$  gets continuously deformed and generates a branch of solutions  $f_n(\psi, \kappa)$ , at least for small values of  $\kappa$ . For  $n = 2$  the solution exists on the interval

$$0 \leq \kappa^2 \leq \kappa_{cr}^2(2) \quad ; \quad \kappa_{cr}^2(2) \simeq 0.261 \quad (15)$$

$$E_2(\kappa_{cr}^2(2))/6\pi^2 \simeq 1.670 \quad (16)$$

The profile of  $f_2(\psi, \kappa_{cr}^2(2))$  is also shown on Fig.1 and the energy of the solution is represented (in function of  $\kappa$ ) by the upper part of the  $n = 2$  curve in Fig.3. We find no solution for  $\kappa^2 > \kappa_{cr}^2$  but a second branch of solutions, say  $\tilde{f}_2(\psi, \kappa^2)$ , exists on the interval (15). For fixed  $\kappa$ , the energy of the solution  $\tilde{f}_2$  is lower than the energy of  $f_2$ , i.e. (using an obvious notation)

$$\tilde{E}_2(\kappa) \leq E_2(\kappa) \quad (17)$$

as represented by the lower and upper branches of the  $n = 2$  curve in Fig.3. At  $\kappa^2 = \kappa_{cr}^2(2)$  the solutions  $f_2$  and  $\tilde{f}_2$  coincide and the energy plot terminates in a cusp shape, suggesting some catastrophic behaviour.

We would like to stress that the evolution of the solution profile from the upper branch to the lowest one is completely smooth, the profiles of the solution  $\tilde{f}_2(\psi, 0.2)$ ,  $\tilde{f}_2(\psi, 0.002)$  are displayed of Fig.1. The numerical analysis strongly suggests (as illustrated by Fig.1) that

$$\lim_{\kappa^2 \rightarrow 0} \tilde{f}_2(\psi, \kappa^2) = \pi \quad \text{for} \quad 0 < \psi < \pi \quad (18)$$

This statement is also supported by the evaluation of the energy

$$\lim_{\kappa^2 \rightarrow 0} \tilde{E}_2(\kappa^2) = E_0(0) = 0. \quad (19)$$

as indicated on Fig.3

Similarly, the branch developping from the  $n = 3$  solution exists on the interval

$$0 \leq \kappa^2 \leq \kappa_{cr}^2(3) \quad ; \quad \kappa_{cr}^2(3) \simeq 0.017 \quad (20)$$

and

$$E_3(\kappa_{cr}^2(3))/6\pi^2 \simeq 1.395 \quad (21)$$

Again the second branch of solutions  $\tilde{f}_3(\psi, \kappa^2)$  occurs and a few of these solutions are superposed on Fig. 2 (resp.  $f_3(\psi, 0)$ ,  $f_3(\psi, \kappa_{cr}^2(3))$ ,  $\tilde{f}_3(\psi, 0.015)$ ,  $\tilde{f}_3(\psi, 0.0005)$ ). The numerical results suggest that

$$\lim_{\kappa^2 \rightarrow 0} \tilde{f}_3(\psi, \kappa^2) = \pi - \psi \quad \text{for} \quad 0 < \psi < \pi \quad (22)$$

to be compared with (13). We also find  $\lim_{\kappa^2 \rightarrow 0} E_3(\kappa^2) = E_1(0) = 6\pi^2$ .

In view of these results, we conjecture that two branches of solutions say,  $f_n(\kappa^2)$  and  $\tilde{f}_n(\kappa^2)$ , exist for  $0 < \kappa^2 < \kappa_{cr}^2(n)$  and that the result suggested by our numerical analysis holds for  $n > 3$ , that is to say

$$\lim_{\kappa \rightarrow 0} \tilde{f}_n(\kappa^2) = f_{n-2}(0) \quad \text{for} \quad 0 < \psi < \pi \quad (23)$$

$$\lim_{\kappa \rightarrow 0} \tilde{E}_n(\kappa^2) = E_{n-2}(0) \quad (24)$$

## 4 Stability

The stability of the solutions constructed in the previous section can be studied by perturbing the classical solution, say  $\bar{f}(\psi)$ . In this paper, we limit ourselves to fluctuations depending only on  $\psi$ , i.e.

$$f(\psi) = \bar{f}(\psi) + \eta(\psi) \quad (25)$$

Expanding the functional (10) in powers of  $\eta$  leads to a quadratic form which can be diagonalized. The relevant eigenvalue equation reads

$$\begin{aligned} & \left[ - \left( 1 + \kappa^2 \frac{\sin^2 \bar{f}}{\sin^2 \psi} \right) \frac{d^2}{d\psi^2} \right. \\ & - \left( 2 \cot \psi - \kappa^2 \bar{f} \frac{\sin 2\bar{f}}{\sin^2 \psi} \right) \frac{d}{d\psi} \\ & + \left( 2 \frac{\cos 2\bar{f}}{\sin^2 \psi} + \kappa^2 (\bar{f}')^2 \frac{\cos 2\bar{f}}{\sin^2 \psi} \right. \\ & \left. \left. + \frac{\kappa^2}{2} \frac{1}{\sin^4 \psi} (\sin^2 2\bar{f} + 2 \sin^2 \bar{f} \cos 2\bar{f}) \right) \right] \eta = \omega^2 \eta \end{aligned} \quad (26)$$

and determines the normal modes  $\eta(\psi), \omega^2$  about the classical solution  $\bar{f}(\psi)$ .

For the vacuum,  $\bar{f}(\psi) = 0$ , this equation becomes independent of  $\kappa^2$  and can be solved explicitly; the normal modes read

$$\eta_k(x) = \sin \psi \ C_k^2(\cos \psi) \ , \ \omega_k^2 = 3 + k(k + 4), \quad (27)$$

with  $k = 0, 1, 2, \dots$  and where  $C_k^2(t)$  denote the Gegenbauer polynomials

$$C_0^2 = 1 \ , \ C_1^2(t) = t, \quad (28)$$

$$(n + 2)C_{n+2}^2(t) = 2(n + 3)tC_{n+1}^2(t) - (n + 4)C_n^2(t) \quad (29)$$

The lowest eigenvalues associated with the solutions  $\bar{f}(\psi) = f_n(\psi, 0)$  are given in [1]. Apart from the case  $n = 1$  whose eigenvector have the form (27) with eigenvalues

$$\omega_k^2 = -1 + k(k + 4) \quad (30)$$

the spectrum has to be computed numerically. In particular the solution  $f_n(\psi, 0)$  possesses  $n$  independent modes of instability of the form (25).

We studied Eq. (26) numerically for  $\kappa^2 > 0$  and for the two modes of lowest eigenvalues associated with the solutions corresponding to  $n = 1$  and  $n = 2$ . Our results are reported on Fig. 4. The solid lines  $a, b$  (resp.  $c, d$ ) represent the modes (27), (resp. (30)) for  $k = 0, 1$ ; we see that the negative mode about  $f_1(\psi, \kappa^2)$  becomes positive for  $\kappa > 0.8$  (this is not sufficient, however, to claim that  $f_1(\psi_1 \kappa^2)$  is a local minimum of (7), general fluctuations have to be considered as well). We also notice that the solution  $\tilde{f}_2(\psi, \kappa^2)$  has no directions of instability in the channel (25).

The two lowest modes relative to the solution  $f_2(\psi, \kappa^2)$  (resp.  $\tilde{f}_2(\psi, \kappa^2)$ ) are represented by the dashed (resp. dotted) lines on Fig. 4. The numerical results strongly support the fact that the lowest modes about the solution  $f_2(\psi, \kappa^2)$  and the solutions  $\tilde{f}_2(\psi, \kappa^2)$  vanish in the limit  $\kappa^2 \rightarrow \kappa_{cr}^2(2)$ . This confirm on an explicit example a general expectation (based on catastrophe theory; see. e.g. [5]) that the solution on the higher branch (i.e.  $\tilde{f}_2$ ) has one more directions of instability than the solution on the lower branch (i.e.  $f_2$ ).

## 5 Conclusions

The non-linear sigma model based on the mapping of  $S^3$  into  $S^3$  admit a rich set of classical solutions [1]. By supplementing it by a Skyrme-like term,

we have shown that the solutions can be interpolated by the extrema of the family of models indexed by the coupling constant  $\kappa^2$ .

The energy of the classical solution then leads to a serrated pattern summarized by Fig. 3. Apart from the two lowest branches, which respectively play the role of the vacuum ( $E = 0$ ) and of the Skyrmion solution of standard Skyrme model, the other solutions cease to exist at critical values of the parameter  $\kappa^2$ , where two branches of solutions terminate into a catastrophic cusp.

The analysis of the normal modes about the different solutions indicates that their stability strongly depends on the Skyrme term and suggests that the spectrum of the quadratic fluctuation operator varies continuously with the parameter  $\kappa^2$ .

**Acknowledgements** We gratefully acknowledge discussions with P. Bizon.

#### Figure Captions

Figure 1 The solution  $f_2(\psi, \kappa^2)/\pi$  is plotted in function of  $\psi/\pi$  for four different values of the coupling constant  $\kappa$ .

Figure 2 The solution  $f_3(\psi, \kappa^2)/\pi$  is plotted in function of  $\psi/\pi$  for four different values of the coupling constant  $\kappa$ .

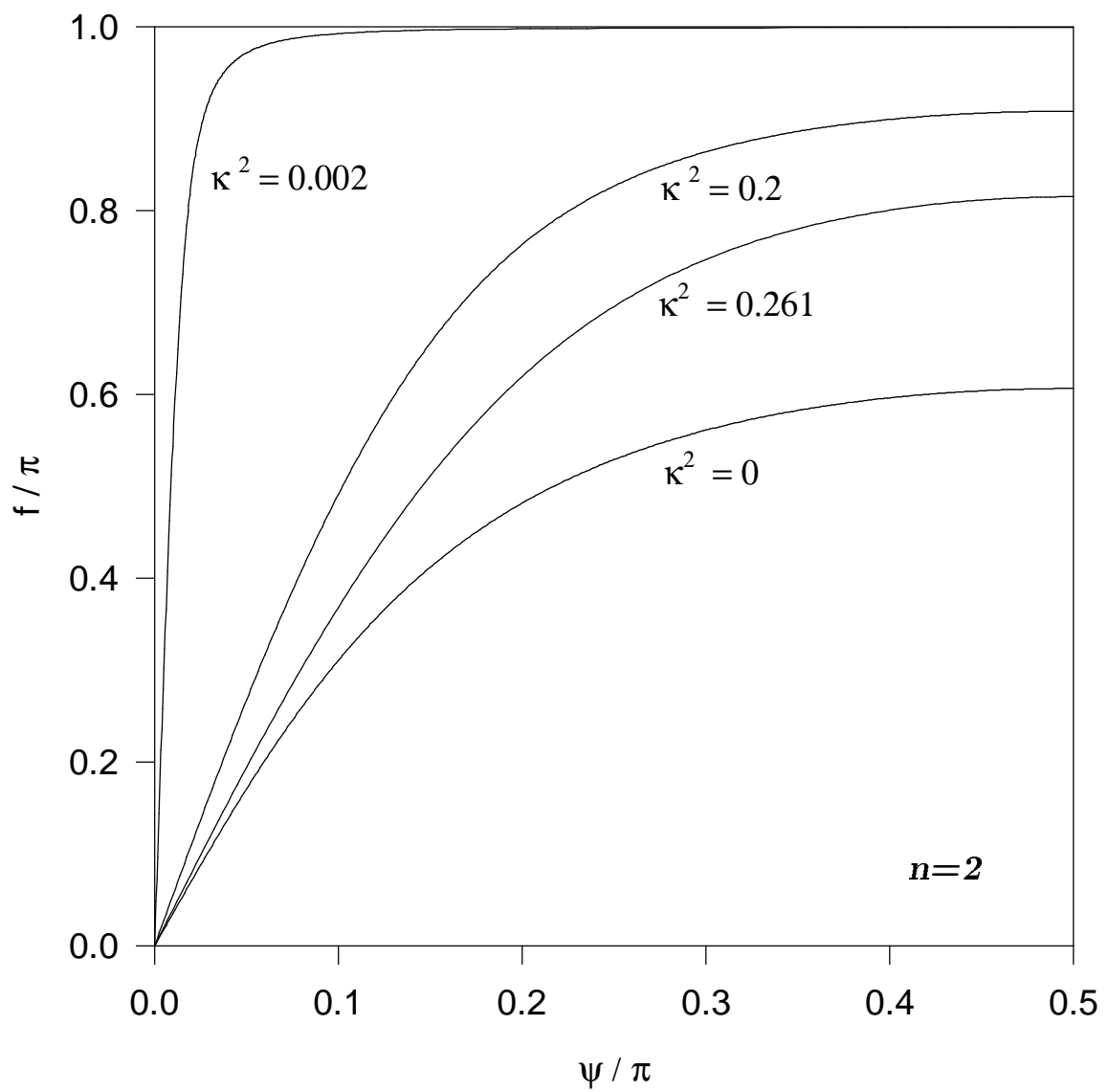
Figure 3 The energy of the solutions corresponding to  $n = 1, 2, 3$  is plotted in function of the coupling constant  $\kappa$ .

Figure 4 Some eigenvalues of Eq.(26) are plotted in function of  $\kappa$ . The lines  $a, b$  refer to the vacuum (27) and the lines  $c, d$  to the  $n = 1$  solution. The dashed (resp. dotted) lines refer to the modes of the solution  $f_2$  (resp.  $\tilde{f}_2$ ).

## References

- [1] P. Bizon, *Harmonic maps between three-spheres*, hep-th/9407140.
- [2] T.H.R. Skyrme, Proc. Roy. Soc. **A260** (1961) 127; Nucl.Phys. 31 (1962) 556.
- [3] J. Boguta and J. Kunz, Phys. Lett. **B166** (1986) 93. J. Kunz and D. Masak, Phys. Lett. **B179** (1986) 176.
- [4] Y. Brihaye and J. Kunz, Mod. Phys. Lett. **A4** (1989) 2723.
- [5] G. Eilam, D. Klabucar and A. Stern, Phys. Rev. Lett. **56** (1986) 1331.
- [6] Y. Brihaye, J. Kunz, C. Semay, Phys. Rev. **B42** (1990) 2846.
- [7] M. Bando et al. Phys. Rev. Lett. **54** (1985) 1215.

*Figure 1*



**Figure 2**

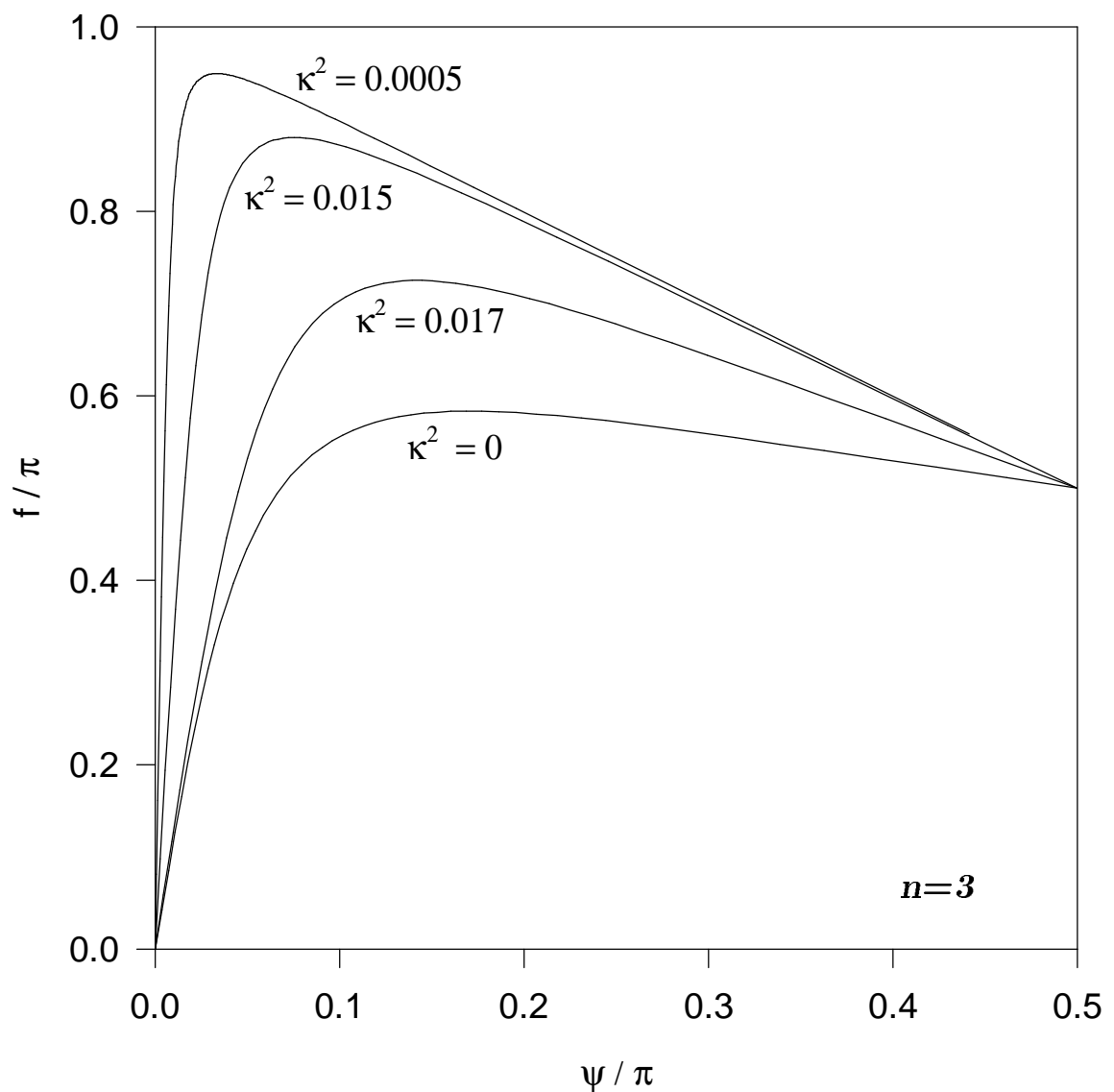


*Figure 3*

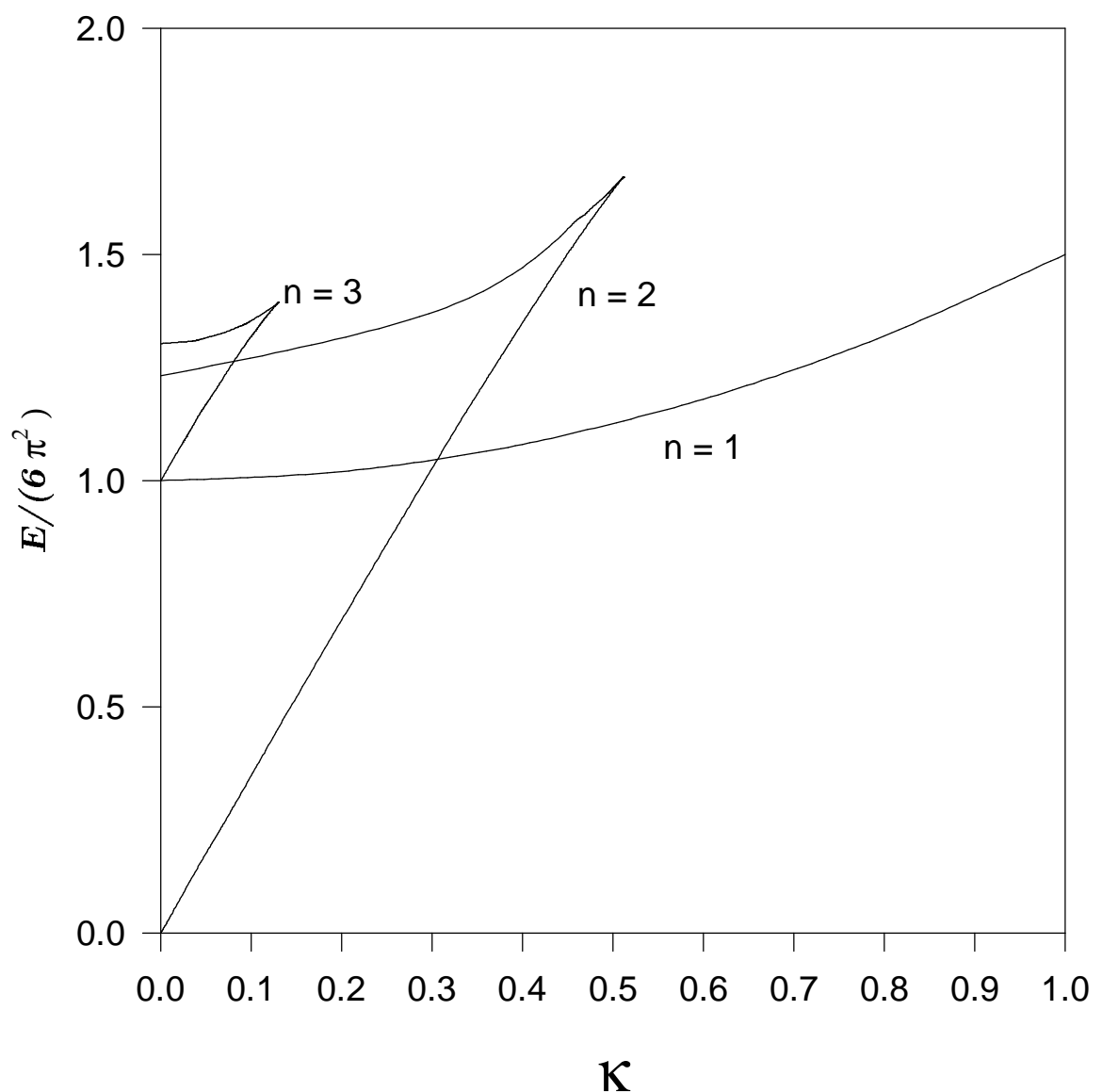


Figure 4

